SCIENTIFIC REPORTS

OPEN

SUBJECT AREAS:
ELECTRONIC MATERIALS
ELECTRONIC DEVICES

Received
22 April 2014

Accepted
6 May 2014

Published
4 June 2014

Correspondence and requests for materials should be addressed to K.-T.W. (kenwong@ntu.edu.tw)

The First Tandem, All-exciplex-based WOLED

Wen-Yi Hung[1], Guan-Cheng Fang[1], Shih-Wei Lin[2], Shuo-Hsien Cheng[2], Ken-Tsung Wong[2,3], Ting-Yi Kuo[2] & Pi-Tai Chou[2,4]

[1]Institute of Optoelectronic Sciences, National Taiwan Ocean University, Keelung, 20224, Taiwan, [2]Department of Chemistry, National Taiwan University, Taipei, 10617, Taiwan, [3]Institute of Atomic and Molecular Sciences, Academia Sinica, Taipei, 10617, Taiwan, [4]Center for Emerging Material and Advanced Devices, National Taiwan University, Taipei, 10617, Taiwan.

Exploiting our recently developed bilayer interface methodology, together with a new wide energy-gap, low LUMO acceptor (A) and the designated donor (D) layers, we succeeded in fabricating an exciplex-based organic light-emitting diode (OLED) systematically tuned from blue to red. Further optimization rendered a record-high blue exciplex OLED with η_{ext} of 8%. We then constructed a device structure configured by two parallel blend layers of mCP/PO-T2T and DTAF/PO-T2T, generating blue and yellow exciplex emission, respectively. The resulting device demonstrates for the first time a tandem, all-exciplex-based white-light OLED (WOLED) with excellent efficiencies η_{ext}: 11.6%, η_c: 27.7 cd A^{-1}, and η_p: 15.8 ml W^{-1} with CIE(0.29, 0.35) and CRI 70.6 that are nearly independent of EL intensity. The tandem architecture and blend-layer D/A (1 : 1) configuration are two key elements that fully utilize the exciplex delay fluorescence, providing a paragon for the use of low-cost, abundant organic compounds en route to commercial WOLEDs.

Recently, to circumvent the high-cost, limited sources, and potential health threats raised by the transition metal complexes incorporated in organic light emitting diodes (OLEDs), two upconversion mechanisms including triplet-triplet annihilation (TTA)[1–3] and thermally activated delay-fluorescence (TADF)[4–9] have been successfully utilized to yield high efficiency OLEDs with tailor-made organic emitters. Particularly, the attainable 100% internal quantum efficiency (IQE) of TADF-based OLEDs has been receiving considerable attention.

A key element for generating efficient TADF lies in the small singlet-triplet energy ΔE_{ST} (<kT), i.e., the small electron exchange energy. This can be achieved, in theory, by having orthogonality or slim overlap between HOMO and LUMO involved in the transition. Accordingly, organic molecules capable of demonstrating TADF are composed of structurally weak-coupled electron donor (D) and acceptor (A) components, inducing an *intramolecular* charge transfer (ICT) behavior. This makes the design of a new D/A molecule to attain efficient TADF a nontrivial matter, one requiring the subtle harnessing of the degree of ICT within the molecular framework. Alternatively, a similar result can be achieved by the formation of exciplex via *intermolecular* charge transfer between physically blended electronic donor and acceptor molecules. The realization of this simplicity has caused a rapid boom in exciplex applications in OLEDs. With the judicious selection of donor and acceptor materials, OLEDs with exceptionally high electroluminescence (EL) efficiencies have been achieved recently[10,11].

While most researchers have utilized a mixed layer for D and A in OLED applications, in a recent contribution, we have seminally demonstrated a record-high ($\eta_{ext} \sim 7.7\%$) bilayer-type exciplex-based OLED by using a triazene-centered electron-transporting (ET) molecule 3P-T2T as acceptor and a carbazole-based hole-transporting (HT) material TCTA as donor[12]. The large offsets of TCTA/3P-T2T energy levels assist the accumulation of charge carriers at the interfacial region for increasing the carrier recombination probability to give S_1 and T_1 exciplex excitons, for which the physical interaction and hence weak D/A coupling results in a very small ΔE_{ST}. As a result, efficient thermally activated $T_1 \rightarrow S_1$ reverse intersystem crossing takes place in the interface, generating the exciplex delay fluorescence that serves as a key for the high performance OLED.

In this contribution, we fully extend the unrecognized potential of this bilayer interface technology. By designing a new acceptor and ingeniously selecting donors, we are capable of fabricating the bilayer, exciplex-based OLEDs systematically fine-tuned from blue to red. With this, we then accomplished a great leap by constructing a tandem structure configured by the two parallel blend layers, generating blue and yellow exciplex emissions simultaneously and consequently an all-exciplex, white light organic light-emitting diode (WOLED) with a record high η_{ext} of 11.6%.

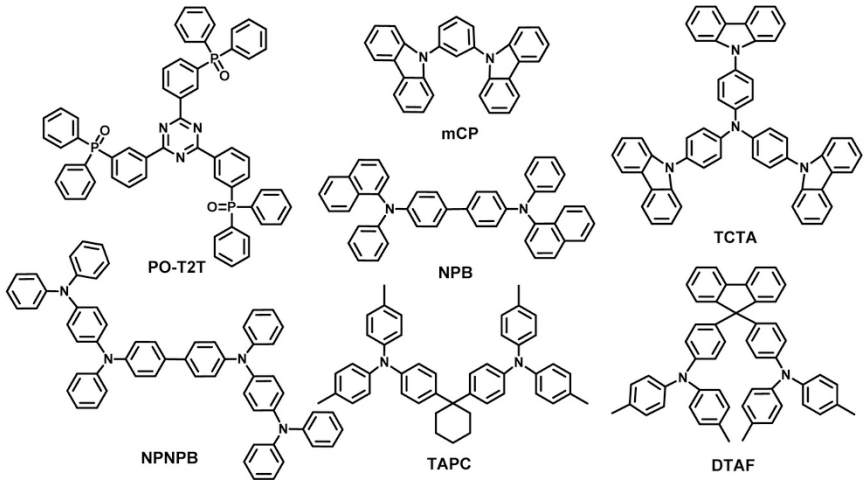

Figure 1 | **Molecular structures of PO-T2T and the donors used in this study.**

To realize the formation of a high-energy exciplex (>2.6 eV), it is essential to have an ET material with a rather low LUMO (HOMO) for the better electron injection (hole-blocking) and high triplet energy to confine the exciplex exciton. Also, this designated ET material should exhibit high electron mobility comparable to the high hole mobility common of HT materials. Recently, triazine-based molecules have emerged as promising ET materials[13–15] as well as host materials for Ir-based phosphors[16–19]. More recently, we have demonstrated a high efficiency yellow exciplex with TCTA as the HT layer and a triazine-based molecule (3P-T2T)[12] as the ET layer. To further reduce the LUMO energy and retain the high triplet energy, we herein introduced diphenylphosphine oxide as the electron-withdrawing group as well as the conjugation-blocking group[20–22] to make a new ET material PO-T2T (Fig. 1) for this work (see Supplementary online information for synthesis/characterization).

PO-T2T exhibits excellent thermal stability, with a high decomposition temperature (T_d) of 460° (5% weight loss) analyzed by thermogravimetric analysis (TGA). No evident glass transition temperature was observed for PO-T2T by differential scanning calorimetry (DSC). In CH_2Cl_2 solution, PO-T2T shows an absorption maximum centered at 272 nm and an emission peak at 405 nm, ascribed to the π-π* transitions of the 1,3,5-triphenyltriazine core (see Supplementary Fig. S1 online). The lowest lying triplet energy (E_T) of PO-T2T was calculated to be 2.99 eV, referring to the highest energy vibronic sub-band of the phosphorescence spectra measured at 77 K (2Me-THF). In addition, one quasi-reversible reduction potential (−1.97 V vs. Fc/Fc^+) of PO-T2T was detected by cyclic voltammetry analysis (see Supplementary Fig. S2 online). This result was used to calculate the LUMO of PO-T2T to be −2.83 eV and the HOMO to be −6.83 eV, with the equation of HOMO = LUMO-E_g

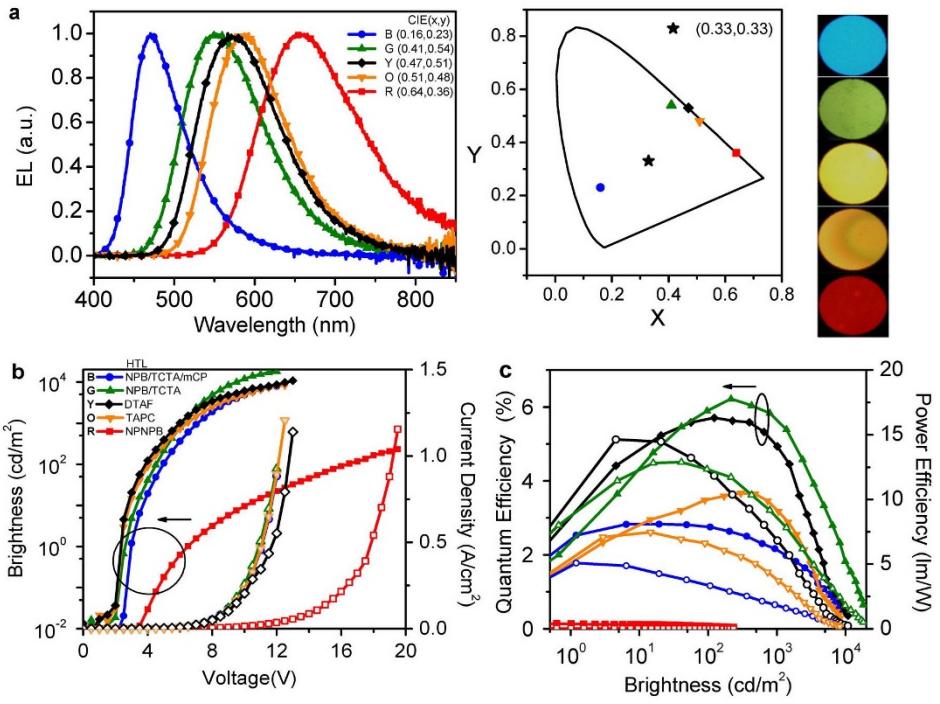

Figure 2 | **Performance characteristics of the OLEDs with different HTL.** (a) EL spectra and CIE coordinate of the devices B, G, Y, O and R exciplex-based OLEDs. (b) Current density-voltage-luminance (*J–V–L*) characteristics. (c) External quantum and power efficiencies as a function of brightness in the structure ITO/PEDOT:PSS/HTL (25 nm)/PO-T2T (75 nm)/Liq/Al.

Table 1 | EL performances of devices

Device	HTL	V_{on} [V][a]	L_{max} [cd/m^2]	I_{max} [mA/cm^2]	η_{ext} [%]	η_c [cd/A]	η_p [lm/W]	at 100 cd m^{-2} [V,%] [b]	CIE [x,y]
B	NPB/TCTA/mCP	2.5	7860 (12 V)	880	2.8	5.4	5.1	5.0, 2.8	0.16,0.23
G	NPB/TCTA	2.0	18100 (12 V)	930	6.2	18.6	12.9	4.5, 5.9	0.41,0.54
Y	DTAF	2.0	10800 (13 V)	1140	5.7	15.1	14.6	3.8, 5.7	0.47,0.51
O	TAPC	2.0	8280 (12.5 V)	1210	3.7	8.9	7.5	4.0, 3.5	0.51,0.48
R	NPNPB	3.0	230 (19.5 V)	1160	0.2	0.1	0.1	16.5, 0.06	0.64,0.36
B1	TAPC/mCP	2.0	24600 (12 V)	1040	8.0	6.1	11.2	4.1, 7.4	0.17,0.23
W		4.0	50300 (24 V)	1090	11.6	27.7	15.8	12, 10.6	0.29,0.35

[a]Turn-on voltage at which emission became detectable.
[b]η_{ext} and driving voltage of device at 100 cd m^{-2}.

where E_g is the optical band gap. The physical data of PO-T2T are summarized as Supplementary Table S1 online.

The intensity of exciplex emission relies on the interfacial charge accumulation densities at the donor/acceptor contacts. Hence, high carrier mobilities may play a role in highly efficient exciplex-based OLEDs to improve the electron-hole capture ability at the interface[23]. Here, we employed ambipolar terfluorene (E3) as the charge-generation layer in the Time-of-Flight (TOF) technique[24] to measure the electron mobility of PO-T2T (see Supplementary Fig. S3 online). As a result, high electron mobility is obtained, which lies in the range of 1.7×10^{-3} to 4.4×10^{-3} cm^2·V^{-1}·s^{-1} for fields varying from 8.6×10^5 to 1.2×10^6 V·cm^{-1}.

Exciplex emission is caused by the radiative electronic transition from the LUMO of an acceptor to the HOMO of a donor. Hence, an appropriate selection of the donors (with different HOMO levels) combined with PO-T2T to tune the color from blue to red is crucial to proving the concept. Based on the above results, we selected 1,3-bis(*N*-carbazolyl)benzene mCP (−6.1 eV for blue, **B**)[25], 4,4′,4″-tri(*N*-carbazolyl)triphenylamine TCTA (−5.62 eV for green, **G**)[26], 9,9-di[4-(di-*p*-tolyl)aminophenyl]fluorine DTAF (−5.31 eV for yellow, **Y**)[27], 1,1-bis[(di-4-tolylamino)phenyl]cyclohexane TAPC (−5.3 eV for orange, **O**)[28], and *N*,*N*′-diphenyl-*N*,*N*′-di-[4-(*N*,*N*-diphenyl-amino)phenyl]benzidine NPNPB (−5.16 eV for red, **R**)[29], respectively, as donors in the device structure: ITO/polyethylene dioxythiophene: polystyrene sulfonate (PEDOT:PSS, 30 nm)/HTL (25 nm)/PO-T2T (75 nm)/8-quinolinolato lithium (Liq, 0.5 nm)/Al. In order to smooth the hole injection to mCP/PO-T2T and TCTA/PO-T2T interfaces, the corresponding HTLs are fabricated by NPB (15 nm)/TCTA (5 nm)/mCP (5 nm) and NPB(20 nm)/TCTA (5 nm), respectively.

The chemical structures of titled donors are depicted in Fig. 1, and relevant schematic energy level diagrams relative to **PO-T2T** are shown in Supplementary Fig. S4 online. The physical properties of the donors are also shown in Supplementary Fig. S5–6 online. Fig. 2a reveals the EL spectra and CIE coordinates of the devices **B**, **G**, **Y**, **O** and **R** OLEDs with the corresponding emission peak wavelengths at about 471, 552, 572, 586, and 657 nm, respectively. Each of the EL spectra does not correspond to any monomer emission, indicating that it originates from interfacial electron–hole recombination between the donor (HOMO, hole) and acceptor (LUMO, electron) in a form of intermolecular exciplex. This confirms our assumption that exciplex forms at donor/**PO-T2T** interfaces and that EL spectra can be harnessed by selecting different HOMO levels of the donor. Fig. 2b,c depicts the current density–voltage–luminance (*J*–*V*–*L*) characteristics and device efficiencies of the devices. The key parameters of devices are summarized in Table 1. The devices showed external quantum efficiencies (η_{ext}) of 2.8 ∼ 6.2%, and low turn-on voltages of 2.0 ∼ 2.5 V, except for device **R**. The low turn on voltage clearly indicates a direct charge injection into the exciplex HOMO–LUMO levels[30].

The low device efficiency in red (device **R**) deserves further investigation. We first considered the inefficient electron and/or hole injection that impedes the charge collection. To gain insight into the charge transfer dynamics, the femtosecond fluorescence up-conversion technique was applied to probe the early electron/hole transfer dynamics. Upon 380 nm pulse excitation (fwhm ∼ 100 fs), as shown in Fig. 3a, the upconverted signal monitored at 450 nm reveals two fast single exponential decay components of 0.6 ps and 4.5 ps. Note that the 450 nm emission, which is supposed to arise from NPNPB(donor) or PO-T2T(acceptor) monomer, is not observable in a steady-state manner for device **R** (Fig. 2a). The lack of monomer

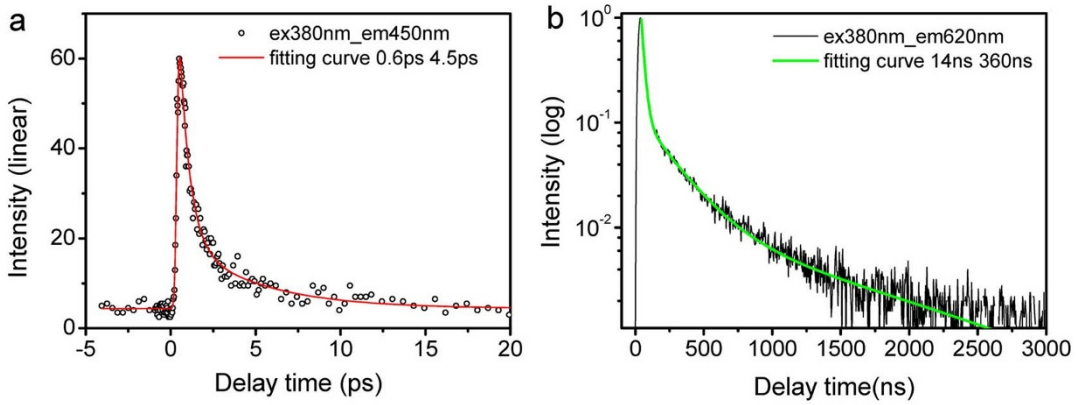

Figure 3 | Transient photoluminescence characteristics. (a) The early dynamics (fluorescence up-conversion) monitored at 450 nm attributed to the monomer emission of either NPNPB or PO-T2T, which is not seen in the steady-state measurement (see Figure 2a, device **R**). Red solid line depicts the best fitting curve by two single exponential decay components (time constants 0.6 ps and 4.5 ps). λ_{ex} = 380 nm. (b) The relaxation dynamics of the exciplex emission monitored at 620 nm for device **R**. The decay was best fitted (green solid line) by two single exponential decay kinetics ($A_1e^{-k_1t} + A_2e^{-k_2t}$) with k_1 = (14 ns)$^{-1}$ (A_1 = 0.91) and k_2 = (360 ns)$^{-1}$(A_2 = 0.09).

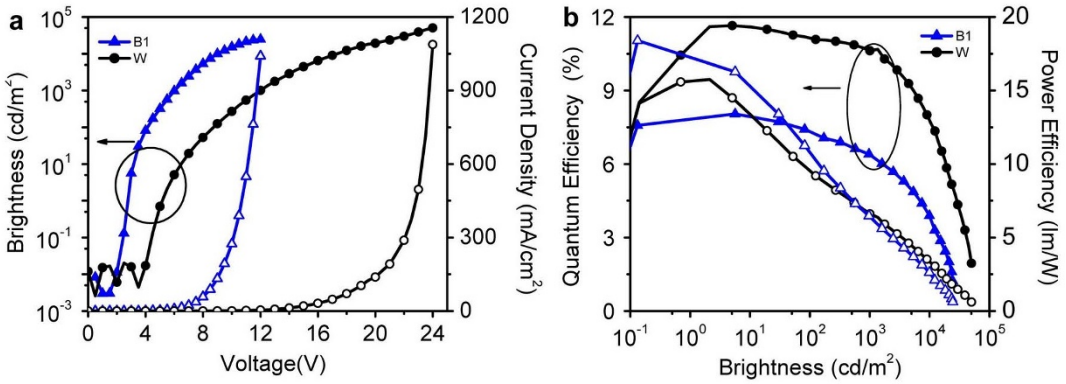

Figure 4 | Performance characteristics of the OLEDs for optimized blue device B1 and tandem device W. (a) Current density-voltage-luminance (*J–V–L*) characteristics. (b) External quantum and power efficiencies as a function of brightness.

emission is consistent with the fast photoinduced electron/hole transfer in the NPNPB(donor)/PO-T2T(acceptor) configuration, generating 650 nm exciplex emission. Since the 380 nm photons are absorbed mainly by NPNPB (see Supplementary Fig. S6 online for the corresponding absorption spectra), it is reasonable to ascribe the major $(0.6\ ps)^{-1}$ component to the rate constant of the electron transfer, while that of the hole transfer is $(4.5\ ps)^{-1}$. Fig. 3b reveals the relaxation dynamics of the 650 nm exciplex emission for device **R**. The decay was best fitted by two-exponential decay kinetics with 14 ns and 360 ns, in which the former is attributed to the fluorescence. The TADF of 360 ns is relatively short compared to that of >μs for exciplex emission commonly observed in the higher energy region[4]. We thus believe that the inferiority of the 650 nm emission for device **R** is mainly due to relatively low emission yield in the red. The quenching of emission is associated with the operation of the energy gap law[31], i.e., the high-frequency vibrational quenching, and perhaps smaller radiative decay rate constant k_r in the red ($k_r \propto \nu^3$ where ν denotes the emission energy gap in frequency)[32].

In an aim to attain efficient electron–hole capture with high probability in the mCP/PO-T2T, we further optimized OLED structures consisting of ITO/PEDOT:PSS (30 nm)/TAPC (20 nm)/mCP (15 nm)/50 mol% mCP:PO-T2T (20 nm)/PO-T2T (45 nm)/Liq (0.5 nm)/Al. As shown in Fig. 4, device **B1** featured a relatively low turn-on voltage of 2 V and a maximum brightness of 24600 cd m^{-2} at 1040 mA cm^{-2} (11 V), with CIE coordinates of (0.17, 0.23). The maximum external quantum (η_{ext}), current (η_c), and power efficiencies (η_p) were 8.0%, 15.5 cd·A^{-1}, and 18.4 lm·W^{-1}, respectively, which are significantly higher than those of device **B** (2.8%, 5.4 cd·A^{-1}, and 5.1 lm·W^{-1}). The η_{ext} value of 8.0% is higher than the limit of η_{ext} in fluorescence-based OLEDs and is superior to the best blue exciplex OLED reported in the literature[33]. The highly efficient exciplex formation at device **B1** is attributable to the balanced holes and electrons in the heterojunction. In addition, the mCP:PO-T2T (1 : 1) mixture layer effectively enhances the intermolecular contact to improve the light-emitting efficiency and hence attain the record high exciplex-based EL efficiencies in blue.

The success of exciplex-based OLEDs fine-tuned from blue to red then encouraged us to explore their pragmatic application en route toward all-exciplex-based WOLEDs. Although this concept has been reported by inserting two blend layers of m-MTDATA:Al(DBM)$_3$ and TPD:Bphen between HTL and ETL[34], the coexistence of exciplex emissions in two blend layers tends to shift the exciton recombination region to a lower energy side, resulting in very low efficiency (~0.1 cd·A^{-1}) and low color stability. To overcome this problem, we made a leap forward by constructing a tandem structure configured by the two parallel blend layers, generating blue and complementary yellow exciplex emissions simultaneously.

The tandem structure was composed of a two individual blend-layer D/A (1 : 1) configuration by a charge generation layer (CGL) configured as: ITO/PEDOT:PSS (30 nm)/TPAC (20 nm)/mCP (15 nm)/mCP:PO-T2T (1 : 1, 20 nm)/PO-T2T (45 nm)/Liq (1 nm)/Al (1 nm)/MoO_3 (5 nm)/DTAF (20 nm)/DTAF:PO-T2T (1 : 1, 20 nm)/PO-T2T (50 nm)/Liq (0.5 nm)/Al (100 nm). Fig. 5(a) shows the electronic level configurations of the tandem WOLED (device **W**), which is based on the CGL of DTAF/MoO_3/Al/Liq layers[35]. In this CGL unit, holes and electrons are generated from the DTAF/MoO_3 interface. The generated charge carriers are extracted out of the CGL and then injected into the adjacent sub-OLEDs. As shown in Fig. 4, device **W** displayed a turn-on voltage of 4.0 V, an L_{max} of 50300 cd·m^{-2} at 24 V (1090 mA cm^{-2}), a maximum η_{ext} of 11.6% corresponding to η_c of

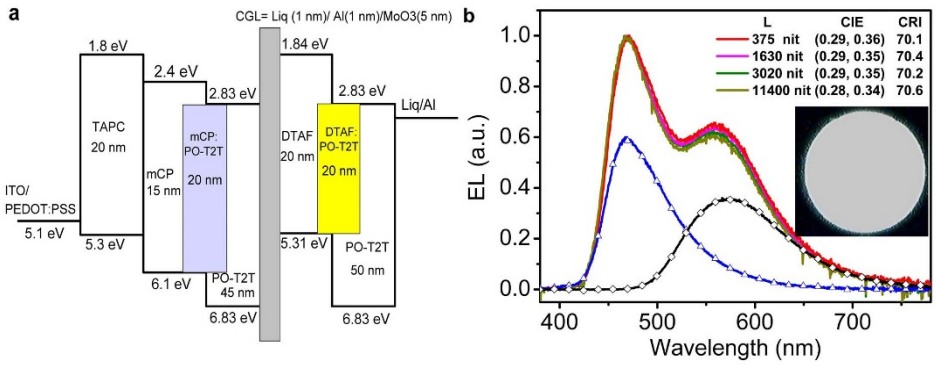

Figure 5 | All-exciplex-based WOLED by tandem structure. (a) The electronic level configurations of tandem WOLED. (b) EL spectra of device **W** at different brightness, and two decomposed bands corresponding to the blue and yellow exciplex emissions.

27.7 cd·A^{-1}, and η_P of 15.8 lm·W^{-1}. The EL spectra of this white device exhibit distinct blue (mCP:PO-T2T) and yellow (DTAF:PO-T2T) exciplex emission bands covering wavelengths from 430 to 730 nm, as shown in Fig. 5(b). Due to the broad exciplex emission band, the color-rendering indices (CRI) of device **W** were calculated to be as high as 70.1–70.6, which are competitive with those of the two-color white OLEDs documented[28]. In addition, the spectra of device **W** also demonstrated highly stable chromaticity (CIEx = 0.28 ~ 0.29 and CIEy = 0.34 ~ 0.36) at different brightnesses (Fig. 5b) and current densities (see Supplementary Fig. S7 online). The tandem architecture with individual emissive units has better color stability and higher efficiency. These superiorities are attributed to the avoidance of the movement of the charge recombination zone and elimination of the energy transfer between blue and yellow emission layers. The performance with a luminance efficiency of 27.7 cd·A^{-1} and color stable white emission is considered to be a quantum leap forward for all-exciplex-based WOLEDs.

In summary, we have developed a new ET compound **PO-T2T** possessing a very low LUMO/HOMO (−2.83/−6.83 eV) and have a proof of concept that a panchromatic range of exciplex emission from blue to red can be attained via systematically tuning the HOMO of the HT material. Based on this, we then demonstrate for the first time a tandem, all-exciplex-based white light organic light-emitting diode (WOLED) with excellent performance. Realizing that $T_1 \rightarrow S_1$ thermally activated delay fluorescence should have IQE of 100%, its utilization to achieve efficient white light generation is still lacking at this stage[36,37]. The tandem architecture and blend layer D/A configuration turned out to be crucial to accounting for the success; otherwise, the electron and hole are too loosely confined to achieve a designated emitting layer. The all-exciplex-delay-fluorescence based tandem WOLED with η_{ext} as high as 11.6% unveiled here is thus truly unprecedented.

1. Kondakov, D. Y. Characterization of triplet-triplet annihilation in organic light-emitting diodes based on anthracene derivatives. *J. Appl. Phys.* **102**, 114504 (2007).
2. Kondakov, D. Y., Pawlik, T. D., Hatwar, T. K. & Spindler, J. P. Triplet annihilation exceeding spin statistical limit in highly efficient fluorescent organic light-emitting diodes. *J. Appl. Phys.* **106**, 124510 (2009).
3. King, S. M. *et al.* The contribution of triplet–triplet annihilation to the lifetime and efficiency of fluorescent polymer organic light emitting diodes. *J. Appl. Phys.* **109**, 074502 (2011).
4. Endo, A. *et al.* Efficient up-conversion of triplet excitons into a singlet state and its application for organic light emitting diodes. *Appl. Phys. Lett.* **98**, 083302 (2011).
5. Lee, S. Y., Yasuda, T., Nomura, H. & Adachi, C. High-efficiency organic light-emitting diodes utilizing thermally activated delayed fluorescence from triazine-based donor–acceptor hybrid molecules. *Appl. Phys. Lett.* **101**, 093306 (2012).
6. Tanaka, H., Shizu, K., Miyazaki, H. & Adachi, C. Efficient green thermally activated delayed fluorescence (TADF) from a phenoxazine–triphenyltriazine (PXZ–TRZ) derivative. *Chem. Commun.* **48**, 11392–11394 (2012).
7. Nakagawa, T., Ku, S.-Y., Wong, K.-T. & Adachi, C. Electroluminescence based on thermally activated delayed fluorescence generated by a spirobifluorene donor–acceptor structure. *Chem. Commun.* **48**, 9580–9582 (2012).
8. Zhang, Q. *et al.* Design of efficient thermally activated delayed fluorescence materials for pure blue organic light emitting diodes. *J. Am. Chem. Soc.* **134**, 14706–14709 (2012).
9. Uoyama, H. *et al.* Highly efficient organic light-emitting diodes from delayed fluorescence. *Nature* **492**, 234–238 (2012).
10. Goushi, K., Yoshida, K., Sato, K. & Adachi, C. Organic light-emitting diodes employing efficient reverse intersystem crossing for triplet-to-singlet state conversion. *Nat. Photon.* **6**, 253–258 (2012).
11. Goushi, K. & Adachi, C. Efficient organic light-emitting diodes through up-conversion from triplet to singlet excited states of exciplexes. *Appl. Phys. Lett.* **101**, 023306 (2012).
12. Hung, W.-Y. *et al.* Highly efficient bilayer interface exciplex for yellow organic light-emitting diode. *ACS Appl. Mater. Interfaces*, **5**, 6826–6831 (2013).
13. Sun, C. *et al.* A polyboryl-functionalized triazine as an electron transport material for OLEDs. *Organometallics* **30**, 5552–5555 (2011).
14. Su, S.-J. *et al.* Tuning energy levels of electron-transport materials by nitrogen orientation for electrophosphorescent devices with an 'ideal' operating voltage. *Adv. Mater.* **22**, 3311–3316 (2010).
15. Inomata, H. *et al.* High-efficiency organic electrophosphorescent diodes using 1,3,5-triazine electron transport materials. *Chem. Mater.* **16**, 1285–1291 (2004).
16. Chen, H.-F. *et al.* Peripheral modification of 1,3,5-triazine based electron-transporting host materials for sky blue, green, yellow, red, and white electrophosphorescent devices. *J. Mater. Chem.* **22**, 15620–15627 (2012).
17. Chang, C.-H. *et al.* A dicarbazole–triazine hybrid bipolar host material for highly efficient green phosphorescent OLEDs. *J. Mater. Chem.* **22**, 3832–3838 (2012).
18. Chen, H.-F. *et al.* 1,3,5-Triazine derivatives as new electron transport–type host materials for highly efficient green phosphorescent OLEDs. *J. Mater. Chem.* **19**, 8112–8118 (2009).
19. Zeng, L., Lee, T. Y.-H., Merkel, P. B. & Chen, S. H. A new class of non-conjugated bipolar hybrid hosts for phosphorescent organic light-emitting diodes. *J. Mater. Chem.* **19**, 8772–8781 (2009).
20. Han, C. *et al.* Short-axis substitution approach selectively optimizes electrical properties of dibenzothiophene-based phosphine oxide hosts. *J. Am. Chem. Soc.* **134**, 19179–19188 (2012)
21. Jeon, S. O. & Lee, J. Y. Phosphine oxide derivatives for organic light emitting diodes. *J. Mater. Chem.* **22**, 4233–4243 (2012).
22. Chou, H.-H. & Cheng, C.-H. A highly efficient universal bipolar host for blue, green, and red phosphorescent OLEDs. *Adv. Mater.* **22**, 2468–2471 (2010).
23. Palilis, L. C., Mäkinen, A. J., Uchida, M. & Kafafi, Z. H. Highly efficient molecular organic light-emitting diodes based on exciplex emission. *Appl. Phys. Lett.* **82**, 2209 (2003).
24. Hung, W.-Y. *et al.* Employing ambipolar oligofluorene as the charge-generation layer in time-of-flight mobility measurements of organic thin films. *Appl. Phys. Lett.* **88**, 064102 (2006).
25. Holmes, R. J. *et al.* Blue organic electrophosphorescence using exothermic host–guest energy transfer. *Appl. Phys. Lett.* **82**, 2422–2424 (2003).
26. Ikai, M. *et al.* Highly efficient phosphorescence from organic light-emitting devices with an exciton-block layer. *Appl. Phys. Lett.* **79**, 156–158 (2001).
27. Hung, W.-Y. *et al.* A new benzimidazole/carbazole hybrid bipolar material for highly efficient deep-blue electrofluorescence, yellow–green electrophosphorescence, and two-color-based white OLEDs. *J. Mater. Chem.* **45**, 10113–10119 (2010).
28. Tang, C. W. & VanSlyke, S. A. Organic electroluminescent diodes. *Appl. Phys. Lett.* **51**, 913 (1987).
29. Adachi, C., Nagai, K. & Tamoto N. Molecular design of hole transport materials for obtaining high durability in organic electroluminescent diodes. *Appl. Phys. Lett.* **66**, 2679–2681 (1995).
30. Morteani, A. C. *et al.* Barrier-free electron–hole capture in polymer blend heterojunction light-emitting diodes. *Adv. Mater.* **15**, 1708–1712 (2003).
31. Englman, R. & Jortner J. The energy gap law for radiationless transitions in large molecules. *J. Mol. Phys.* **18**, 145–164 (1970).
32. Turro, N. J., Ramamurthy, V. & Scaiano, J. C. *Modern Molecular Photochemistry of Organic Molecules.* 195–197 (University Science Books, Sausalito, California, 2010).
33. Jankus, V., Chiang, C.-J., Dias, F. & Monkman, A. P. Deep blue exciplex organic light-emitting diodes with enhanced efficiency; P-type or E-type triplet conversion to singlet excitons? *Adv. Mater.* **25**, 1455–1459 (2013).
34. Zhu, J. *et al.* Very broad white-emission spectrum based organic light-emitting diodes by four exciplex emission bands. *Opt. Lett.* **34**, 2946–2948 (2009).
35. Sasabe, H. *et al.* Ultra high-efficiency multi-photon emission blue phosphorescent OLEDs with external quantum efficiency exceeding 40%. *Org. Electron.* **13**, 2615–2619 (2012).
36. Zhu, H. *et al.* White organic light-emitting diodes via mixing exciplex and electroplex emissions. *Synth. Met.* **159**, 2458–2461 (2009).
37. Lee, K. S., Choo, D. C. & Kim, T. W. White organic light-emitting devices with tunable color emission fabricated utilizing exciplex formation at heterointerfaces including m-MDATA. *Thin Solid Films* **519**, 5257–5259 (2011).

Acknowledgments

This study was supported financially by the National Science Council of Taiwan (NSC 100-2112-M-019-002-MY3, 101-2113-M-002-009-MY3, 101-2628-M-002-008, 102-2633-M-002-001).

Author contributions

K.-T.W., S.-W.L. and S.-H.C. conducted the design, synthesis, and characterizations of PO-T2T. W.-Y.H. and G.-C.F. carried out the OLED device fabrication, measurement, and data analysis. P.-T.C. and T.-Y.K. performed PL decay dynamics and provided the necessary consultations during the write-up of the present article.

Additional information

Supplementary information accompanies this paper at http://www.nature.com/scientificreports

Competing financial interests: The authors declare no competing financial interests.

How to cite this article: Hung, W.-Y. *et al.* The First Tandem, All-exciplex-based WOLED. *Sci. Rep.* **4**, 5161; DOI:10.1038/srep05161 (2014).